Available online at www.sciencedirect.com
SCIENCE DIRECT®
Journal of Organometallic Chemistry 690 (2005) 1889–1900
Journal of Organometallic Chemistry
www.elsevier.com/locate/jorganchem

Syntheses and structural characterizations of rhenium carbonyl complexes of a bitopic ferrocene-linked bis(pyrazolyl)methane ligand

Daniel L. Reger *, Kenneth J. Brown, James R. Gardinier, Mark D. Smith

Department of Chemistry and Biochemistry, University of South Carolina, Columbia, SC 29208, USA

Received 30 August 2004; accepted 25 October 2004
Available online 7 February 2005

Abstract

The reaction between $Fe[C_5H_4CH(pz)_2]_2$ (pz = pyrazolyl ring) and two equivalents of $Re(CO)_5Br$ in refluxing toluene produces $Fe[C_5H_4CH(pz)_2Re(CO)_3Br]_2$ (**1**) in high yield. A similar reaction with a ligand/rhenium ratio of slightly greater than one yields mainly **1** and a low yield of $Fe[C_5H_4CH(pz)_2Re(CO)_3Br][C_5H_4CH(pz)_2]$ (**2**). The compound $H_2C(pz)_2Re(CO)_3Br$ (**3**) was prepared by the reaction of $H_2C(pz)_2$ and $Re(CO)_5Br$. Compounds **1** and **2** show a reversible oxidation at ca. 0.9 V (Ag/AgCl) that can be assigned to the oxidation of the ferrocene moiety and one irreversible oxidation at ca. 1.4 V assigned to the oxidation of the rhenium metal center. The solid-state structures of $\mathbf{1}\cdot CH_3NO_2$, $\mathbf{1}\cdot 2CH_3NO_2$, $\mathbf{1}\cdot 2CH_3CN$ and $\mathbf{2}\cdot 1/2Et_2O\cdot 1/2C_3H_6O$ have been determined, with $\mathbf{1}\cdot 2CH_3NO_2$ and $\mathbf{1}\cdot 2CH_3CN$ being isomorphous. All four are organized into supramolecular structures by the interactions of the acidic hydrogens of the pyrazolyl and methine groups with either the bromine atoms or carbonyl ligand oxygen atoms, and in **2** the lone pairs on the uncomplexed bis(pyrazolyl)methane units.

Keywords: Nitrogen-donor ligands; Rhenium; Ferrocene; Bis(pyrazolyl)methane ligands

1. Introduction

We have recently been developing compounds that show unique supramolecular structures supported by semirigid, multitopic ligands based on linking poly(pyrazolyl)methane units in a single molecule [1]. As part of these studies, we have reported the synthesis of the first ferrocene-linked bis(pyrazolyl)methane ligand, 1,1′-bis(dipyrazol-1-ylmethyl)ferrocene ($Fe[C_5H_4CH(pz)_2]_2$, pz = pyrazolyl ring) and its coordination chemistry with silver(I) [1a]. The ferrocenyl central core has proven to be an excellent choice for incorporation into polymers and coordination network solids because of its interesting electrochemical properties and its ability to provide structural diversity as a result of conformational flexibility [2]. The silver (I) compounds of $Fe[C_5H_4CH(pz)_2]_2$ were found to form either helical or non-helical coordination polymers depending upon the anions and solvents of crystallization. The silver(I) coordination networks were organized into supramolecular structures in the solid state by cooperative $\pi\cdots\pi$, $CH\cdots\pi$, and weak hydrogen bonding interactions.

To further investigate the chemistry of this $Fe[C_5H_4CH(pz)_2]_2$ ligand, a study of its chemistry with the rhenium carbonyl unit $Re(CO)_3Br$ has been carried out. This group should display chemistry very different from that reported earlier because the additional non-labile ligands on the rhenium prevent the formation of coordination polymers. Reported here are the preparations and characterizations of the complexes $Fe[C_5H_4CH(pz)_2Re(CO)_3Br]_2$ (**1**) and $Fe[C_5H_4CH(pz)_2$-$Re(CO)_3Br][C_5H_4CH(pz)_2]$ (**2**) and the details of their solid-state structures. Also reported is the synthesis of $H_2C(pz)_2Re(CO)_3Br$ (**3**) and the electrochemical properties of the new complexes.

* Corresponding author. Tel.: +1 8037772587; fax: +1 8037779521.
E-mail address: reger@mail.chem.sc.edu (D.L. Reger).

0022-328X/$ - see front matter © 2004 Elsevier B.V. All rights reserved.
doi:10.1016/j.jorganchem.2004.10.048

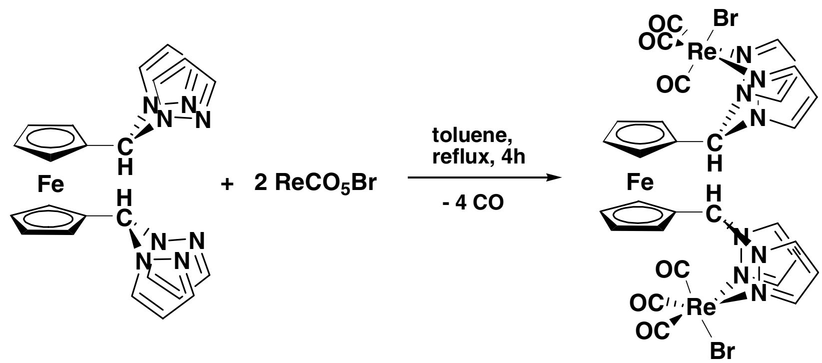

Scheme 1.

2. Results and discussion

2.1. Syntheses

The reaction between $Fe[C_5H_4CH(pz)_2]_2$ and two equivalents of $Re(CO)_5Br$ in refluxing toluene gives $Fe[C_5H_4CH(pz)_2Re(CO)_3Br]_2$ (**1**) as an air stable yellow solid in high yield, as in Scheme 1. This solid is soluble in acetonitrile, slightly soluble in acetone, methanol, and nitromethane but insoluble in Et_2O, toluene, and hexanes. The ^1H NMR spectrum in d_6-acetone shows one set of signals for the ligand framework that are shifted with respect to the free ligand. The presence of only one set of peaks indicates that only one of the possible stereoisomers is formed in the preparative reaction. Presumably, this isomer is the same as that observed in the solid-state structure (vide infra), with a *fac* arrangement of the carbonyl ligands and the bromine and methine hydrogen on the same side of the ReN_4C chelate ring (Scheme 1). The ESI(+) mass spectrum shows a signal corresponding to the loss of bromide ion and one for a CH_3CN solvate of the resulting cation. The IR spectrum of **1** in CH_3CN shows three bands as expected for a *fac*-tricarbonyl moiety where the E band expected for local C_{3v} symmetry is split into its lower symmetry component by the symmetry of the molecule.

When the reaction is performed with a ligand/rhenium ratio of slightly greater than one (Scheme 2), it was possible to isolate the desired derivative with an open ligating site, namely $Fe[C_5H_4CH(pz)_2Re(CO)_3Br][C_5H_4CH(pz)_2]$, albeit in low yield (8%). The major product (83% based on $Re(CO)_5Br$) of this latter reaction was the dirhenium complex **1**, which precipitated from the reaction mixture. Compound **2** was isolated from the filtrate, which is a mixture of the desired compound and the free ligand (NMR). The ^1H NMR spectrum of **2** in d_6-acetone showed two sets of peaks for the ligand corresponding to the free and complexed portions of the ferrocenyl ligand, resonances that were distinct from the free ligand and dirhenium derivative, repectively. The ESI mass spectrum showed peaks corresponding to the bromide-free monorhenium cation $\{Fe[C_5H_4CH(pz)_2Re(CO)_3][C_5H_4CH(pz)_2]\}^+$, its CH_3CN solvate, and peaks corresponding to the loss of pyrazolyl fragments.

Since $Fe[C_5H_4CH(pz)_2Re(CO)_3Br][C_5H_4CH(pz)_2]$, **2**, can be envisioned as a useful starting material to a variety of heterotrimetallic (Fe/Re/metal) species, the preparative reaction was studied in detail by numerous combined synthetic scale and NMR scale experiments, but no improvements in yield were realized. The results of the experiments did provide useful information

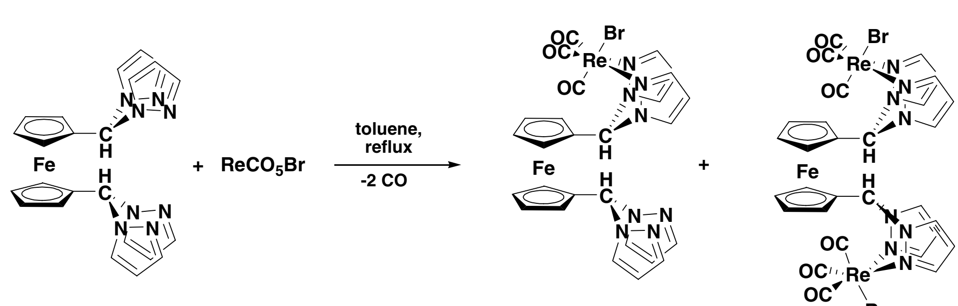

2 **1**

Scheme 2.

regarding the nature of the preparative reaction and the reasons for the low yield of the reaction. First, the reactions carried out in refluxing toluene solutions always produce a mixture of the dirhenium compound **1**, monorhenium compound **2**, and the free ligand, regardless of the stoichiometry. The latter two compounds are soluble in toluene so they can be easily separated from **1** by filtration. The maximum amount of **2** formed in toluene (8%) occurs within 30 min of refluxing an equimolar ratio of starting materials, however, the separation of the monorhenium derivative and the free ligand is difficult as they share similar solubilities in most solvents and the rhenium compound decomposes on silica gel. A greater proportion (29%) of the monorhenium compound is formed and either trace or no dirhenium compound was produced in a reaction using an equimolar ratio of starting material carried out in refluxing acetone, however, difficulties with separating the monorhenium complex from unreacted $Re(CO)_5Br$ and free ligand still limit the ability to enhance the yield of the pure product.

The compound $H_2C(pz)_2Re(CO)_3Br$ (**3**) was prepared by the reaction of $H_2C(pz)_2$ and $Re(CO)_5Br$ for comparison with the electrochemistry of **1** and **2** as below. The ^{1}H NMR spectrum of **3** at ambient temperatures showed the CH_2 group as two broadened doublets, clearly indicating a fluxional process in solution. As shown in Fig. 1, a variable temperature study indicated the presence of two conformers in solution that interconvert slowly on the NMR time scale at low temperatures. As shown previously by an X-ray structure of the dimethyl analog of **3**, $Me_2C(pz)_2Re(CO)_3Br$ [3], these compounds exist in a half-boat configuration with the carbon atom puckered out of the CN_4Re ring. Thus, the two conformers observed in the NMR experiment represent the two forms where the direction of the puckering is either toward the Br or the adjacent CO ligand. Conformers were not observed with $Me_2C(pz)_2Re(CO)_3Br$, presumably the larger methyl groups favor one isomer over the other to a greater extent than with **3**. The energy difference for the two conformers of **3** is 0.58 kcal/mol at 208 K and the equilibrium position is largely independent of temperature. The barrier to the boat flip is 12.5 kcal/mol.

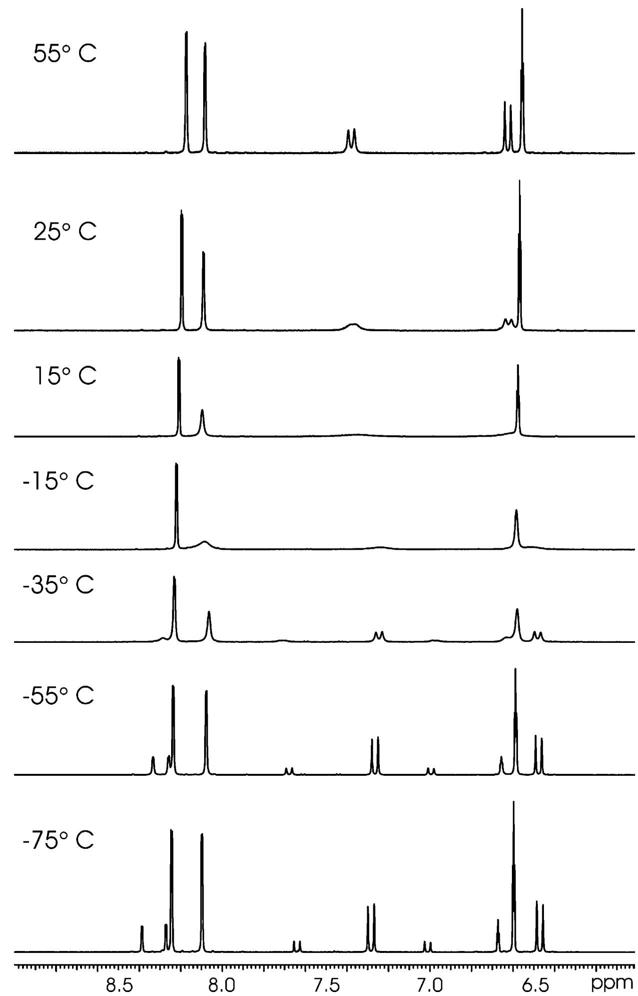

Fig. 1. Variable temperature ^{1}H NMR data for $H_2C(pz)_2Re(CO)_3Br$ (**3**) in acetone-d^6.

2.2. Cyclic voltammetric studies

The measured cyclic voltammetric (CV) data for compounds **1** and **2** are collected in Table 1. As a basis for comparison, the CV data for the uncomplexed ligand $Fe[C_5H_4CH(pz)_2]_2$ [1a], $H_2C(pz)_2Re(CO)_3Br$ and $Me_2C(pz)_2Re(CO)_3Br$ [3] are also recorded. The cyclic voltammogram for the uncomplexed ligand (Fig. 2(a)) exhibits one irreversible oxidation at 0.61 V that can be assigned to the ferrocene moiety. Compound **1** (Fig. 2(b)) shows one reversible oxidation at 0.91 V that can be assigned to the oxidation of the ferrocene moiety and one irreversible oxidation at 1.40 V. The latter wave is the result of oxidation of the rhenium metal center based on the data for compounds $H_2C(pz)_2Re(CO)_3Br$ (**3**) and $Me_2C(pz)_2Re(CO)_3Br$, which do not contain a ferrocene moiety, and the fact that these values are consistent with those previously reported in the literature [4]. Compound **2** also shows two oxidation waves at 0.89 V (reversible) and 1.35 V (irreversible) that can be similarly assigned as in **1**.

Table 1
Reduction potentials (vs Ag/AgCl) of compounds **1**,**2**, the uncomplexed ligand $Fe[C_5H_4CH(pz)_2]_2$, $H_2C(pz)_2Re(CO)_3Br$, and $Me_2C(pz)_2Re(CO)_3Br$

	$E_{1/2}$ (V) vs Ag/AgCl	
$Fe[C_5H_4CH(pz)_2Re(CO)_3Br]_2$ (**1**)	+1.40	+0.91
$Fe[C_5H_4CH(pz)_2Re(CO)_3Br]$-$[C_5H_4CH(pz)_2]$ (**2**)	+1.35	+0.89
$Fe[C_5H_4CH(pz)_2]_2$	–	+0.61
$H_2C(pz)_2Re(CO)_3Br$ (**3**)	+1.37	–
$Me_2C(pz)_2Re(CO)_3Br$	+1.35	–

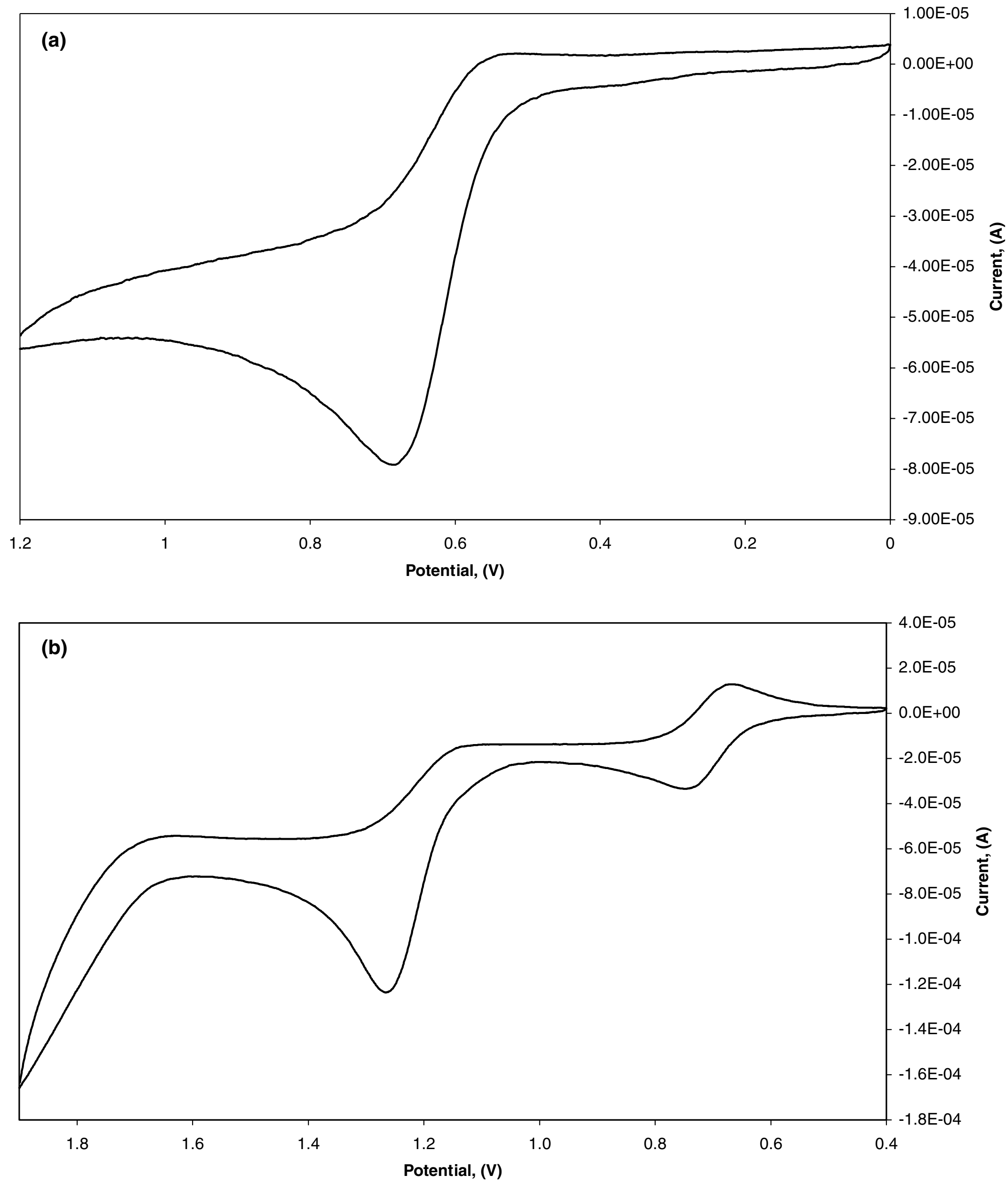

Fig. 2. Cyclic voltammogram for the free ligand, $Fe[C_5H_4CH(pz)_2]_2$ (a), and for compound **1**, $Fe[C_5H_4CH(pz)_2Re(CO)_3Br]_2$ (b).

2.3. Solid-state structures

Compounds **1** and **2** were crystallized by a variety of vapor-phase diffusion techniques (see Section 4). In the case of **1**, vapor-phase diffusion of diethyl ether into a nitromethane solution led to the formation of two crystalline forms, containing either one or two CH_3NO_2 molecules of crystallization. Fig. 3 shows an ORTEP diagram of $\mathbf{1}\cdot CH_3NO_2$, and the atom-numbering scheme shown is applicable to all three crystalline forms of **1**: $\mathbf{1}\cdot CH_3NO_2$, $\mathbf{1}\cdot 2CH_3NO_2$, or $\mathbf{1}\cdot 2CH_3CN$. Fig. 4 shows an ORTEP diagram of $\mathbf{2}\cdot 1/2Et_2O\cdot 1/2C_3H_6O$. Selected bond distances and angles for all four structures are given in Table 2.

The rhenium atoms in the solid-state structures of $\mathbf{1}\cdot CH_3NO_2$, $\mathbf{1}\cdot 2CH_3NO_2$, $\mathbf{1}\cdot 2CH_3CN$, and $\mathbf{2}\cdot 1/2Et_2O\cdot 1/2C_3H_6O$ are in distorted octahedral environments and are surrounded by two nitrogen atoms from the two pyrazolyl rings, three carbon atoms from the carbonyl ligands (facial arrangement), and a bromine atom. The Re–N bond distances for the complexes are similar with the average Re–N distances for $\mathbf{1}\cdot CH_3NO_2$, $\mathbf{1}\cdot 2CH_3NO_2$, and $\mathbf{1}\cdot 2CH_3CN$ of 2.18, 2.17, and 2.17 Å, respectively, the distance for $\mathbf{2}\cdot 1/2Et_2O\cdot 1/2C_3H_6O$ is slightly longer at 2.19 Å. These distances are similar to those for $Me_2C(pz)_2Re(CO)_3Br$ as previously reported [3]. Interestingly, in each of the rhenium complexes, one carbonyl ligand from each rhenium center is directly

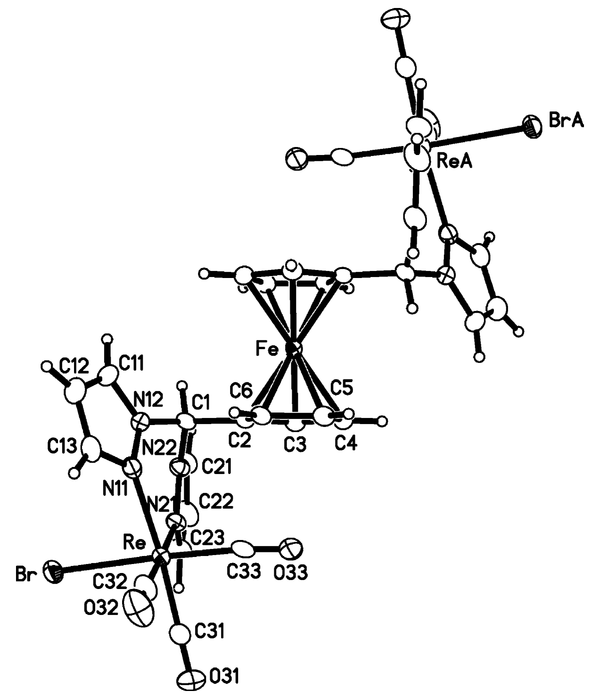

Fig. 3. ORTEP diagram of $1 \cdot CH_3NO_2$. Displacement ellipsoids are drawn at the 50% probability level. The atom-numbering scheme shown is also correct for $1 \cdot 2CH_3NO_2$ and $1 \cdot 2CH_3CN$.

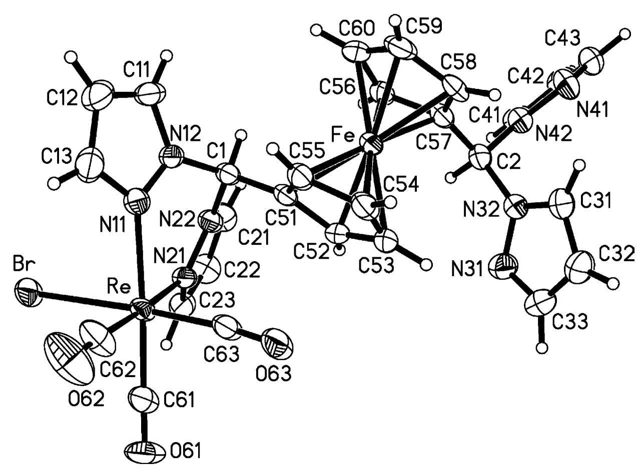

Fig. 4. ORTEP diagram of $2 \cdots 1/2Et_2O \cdot 1/2C_3H_6O$. Displacement ellipsoids are drawn at the 50% probability level.

over and nearly parallel to the Cp ring of the ferrocene unit. It is unclear whether this arrangement is a result of a non-covalent π–π interaction or simply a result of the structural motif.

As a basis for comparison of the orientations of the bis(pyrazolyl)methane units, two torsion angles will be discussed. The first torsion angle, τ_1, is a measure of the rotation of the H(1)–C(1) (or H(2)–C(2)) bond out of the plane of the cyclopentadienyl (Cp) ring to which it is attached, Fig. 5. The second torsion angle, τ_2, determines the rotation of the bis(pyrazolyl)methane units on the Cp rings of the ferrocene unit about the Cp(centroid)–Fe–Cp(centroid) axis [2a], Fig. 6. The angles τ_1 and τ_2 were determined using "ORTEP-3 for Windows version 1.076" [5], and the signs are based on the conventions within the program.

Table 3 contains the τ_1 and τ_2 values for **1** and **2**, as well as a summary of the values for the previously reported silver (I) compounds [1a]. The τ_1 values for $1 \cdot CH_3NO_2$, $1 \cdot 2CH_3NO_2$, and $1 \cdot 2CH_3CN$ (each symmetry equivalent), 66°, 78°, and 78°, respectively, are similar to those of the silver complexes described earlier, which range from 63–72°. Compound $2 \cdot 1/2Et_2O \cdot 1/2C_3H_6O$ has very different τ_1 values for its complexed and uncomplexed sides. The segment of the molecule that contains the complexed rhenium atom has a τ_1 value of 84°, a value similar to those for the solvates of **1**, while the segment containing the uncomplexed pz rings has a τ_1 value of 25°, a value similar to that of the free ligand (avg. 31°). The larger τ_1 angles orient the pyrazolyl rings above the planes of the Cp rings, away from the iron center, reducing steric interactions.

Compound $1 \cdot CH_3NO_2$ has its bis(pyrazolyl)methane moieties in an antiperiplanar staggered orientation [2a], and it is the first complex prepared with this ligand to have a τ_2 value of 180°. This τ_2 value is also observed in the uncomplexed ligand. Compounds $1 \cdot 2CH_3NO_2$ and $1 \cdot 2CH_3CN$ have τ_2 values of 136° and compound $2 \cdot 1/2Et_2O \cdot 1/2C_3H_6O$ has a τ_2 value of 116°. All of these values fall between the ranges of the anticlinal staggered (108°) and anticlinal eclipsed (144°) arrangements. The silver complexes reported previously had lower values of 88° and 94°. With this ligand system, it clear that the large τ_1 angles observed when the ligand arms are complexed to a metal reduce the steric interactions such that τ_2 can take on a large range of values.

2.4. Supramolecular structure of $1 \cdot CH_3NO_2$

The molecules of $1 \cdot CH_3NO_2$ are organized into two-dimensional sheets in the crystallographic *ab*-plane by C–H···Br weak hydrogen bonding interactions (Fig. 7). Hydrogen atoms, H(5) and H(5a), of the Cp rings of one molecular unit are directed toward the bromine atoms of two adjacent molecules. This interaction has an H···Br distance (corresponding angle) of 2.92 Å (138°). The two-dimensional sheets are arranged in a three-dimensional array by C–H···O weak hydrogen bonding interactions. The H(4) and H(4a) hydrogen atoms of the Cp rings of a molecule in one sheet are directed toward a carbonyl ligand oxygen atom, O(33), from a molecule in a neighboring sheet (Fig. 8). This interaction has an H···O distance (corresponding angle) of 2.50 Å (159°). Both hydrogen bonding interactions are within the sum of their van der Waals radii (2.98 Å for H···Br, 2.68 Å for H···O) [6]. The disordered CH_3NO_2 molecules are trapped between the sheets, but have been omitted for clarity.

Table 2
Selected bond distances (Å) and bond angles (°) for compounds **1** · CH_3NO_2, **1** · $2CH_3NO_2$, **1** · $2CH_3CN$, and **2** · $1/2Et_2O$ · $1/2C_3H_6O$

	1·CH_3NO_2	**1**·$2CH_3NO_2$	**1**·$2CH_3CN$	**2**·$1/2Et_2O$·$1/2C_3H_6O$
Re–N(11)	2.177(3)	2.175(3)	2.175(3)	2.190(3)
Re–N(21)	2.176(3)	2.174(3)	2.172(3)	2.184(3)
Re–C(31),C(61)	1.912(4)	1.898(4)	1.907(4)	1.912(4)
Re–C(32),C(62)	1.913(4)	1.914(4)	1.922(4)	1.899(5)
Re–C(33),C(63)	1.929(4)	1.938(4)	1.917(4)	1.907(4)
Re–Br	2.6381(4)	2.6382(4)	2.6381(4)	2.6441(4)
N(11)–Re–N(21)	84.27(10)	86.03(11)	86.01(11)	83.29(11)
N(11)–Re–C(31),C(61)	174.14(13)	174.95(14)	174.75(15)	174.16(14)
N(11)–Re–C(32),C(62)	94.17(14)	91.03(14)	89.90(14)	95.43(17)
N(11)–Re–C(33),C(63)	98.83(12)	96.95(13)	97.27(13)	98.16(14)
N(11)–Re–Br	83.97(7)	85.17(7)	85.51(8)	84.50(8)
N(21)–Re–C(31),C(61)	93.10(13)	93.16(15)	93.92(15)	93.00(15)
N(21)–Re–C(32),C(62)	178.37(13)	175.58(13)	174.25(14)	176.85(16)
N(21)–Re–C(33),C(63)	93.60(13)	93.75(13)	93.82(13)	96.36(15)
N(21)–Re–Br	85.74(7)	84.74(8)	83.93(8)	85.85(8)
C(31),C(61)–Re–C(32),C(62)	88.41(16)	89.48(17)	89.78(17)	88.1(2)
C(31),C(61)–Re–C(33),C(63)	86.54(14)	88.07(16)	87.98(17)	86.70(17)
C(31),C(61)–Re–Br	90.62(11)	89.79(12)	89.26(13)	90.75(11)
C(32),C(62)–Re–C(33),C(63)	87.11(15)	89.88(15)	90.70(16)	86.66(19)
C(32),C(62)–Re–Br	93.63(10)	91.73(11)	91.74(12)	91.18(14)
C(33),C(63)–Re–Br	177.05(10)	177.31(11)	176.30(10)	176.71(11)

The atoms C(61), C(62), and C(63) are the carbonyl ligand carbon atoms for **2**· · ·$1/2Et_2O$· · ·$1/2C_3H_6O$.

2.5. Supramolecular structure of *1·2CH3NO2*

The molecular units of **1**·$2CH_3NO_2$ are arranged into chains by CH· · ·Br interactions (Fig. 9). The acidic methine protons, H(1) and H(1a), of one unit are directed toward the bromine atoms of the two adjacent units. This interaction has an H· · ·Br distance of 2.81 Å (149°). The chains are also supported by a second set of CH· · ·Br interactions between the hydrogen atoms, H(4) and H(4a), of the Cp rings from one unit and the bromine atoms of two neighboring units with an H· · ·Br distance of 2.96 Å (171°).

The chains are organized into a three-dimensional array via a series of CH· · ·O interactions. Fig. 10 shows five chains (orthogonal view to that shown in Fig. 9) that comprise the three-dimensional network. Pyrazolyl ring hydrogen atoms, H(22) and H(22a), from one chain are aimed at the carbonyl oxygen atoms, O(31) and O(31a), from adjacent chains, at an H· · ·O distance of 2.44 Å (172°). The supramolecular structure is organized such that each chain is "connected" to its four neighboring diagonal chains.

The CH_3NO_2 solvent molecules, shown as black spheres in Fig. 10, are highly ordered and participate in CH· · ·O weak hydrogen bonding interactions that

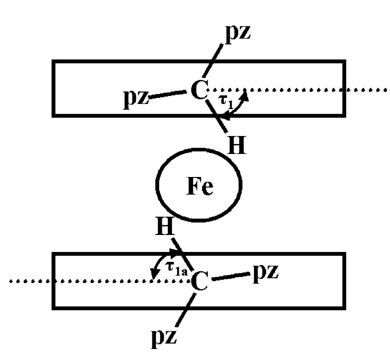

Fig. 5. The torsion angle τ_1 is a measure of the rotation of the C–H bond out of the plane of the Cp ring to which it is attached.

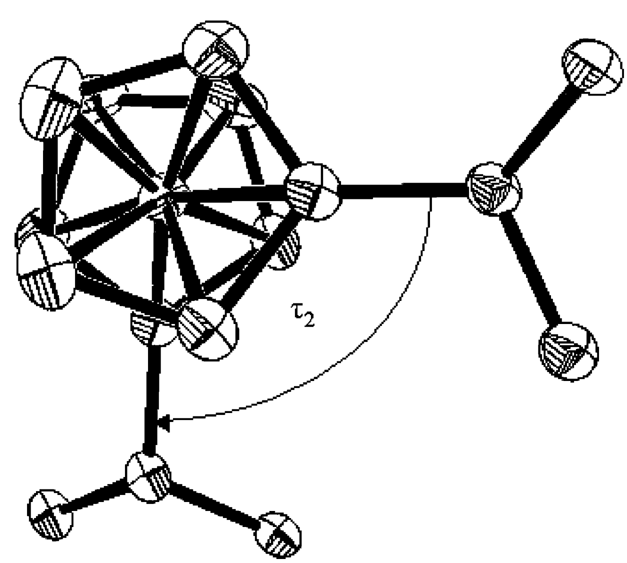

Fig. 6. The torsion angle τ_2 is a measure of the rotation of the bis(pyrazolyl)methane units about the Cp(centroid)–Fe–Cp(centroid) axis.

Table 3
Values of τ_1 (°) and τ_2 (°) for compounds **1** · CH_3NO_2, **1** · $2CH_3NO_2$, **1** · $2CH_3CN$, and **2** · $1/2Et_2O$ · $1/2C_3H_6O$

	τ_1 (°)	τ_2 (°)
1·CH_3NO_2	−66, 66	180
1·$2CH_3NO_2$	78, 78	−136
1·$2CH_3CN$	78, 78	−136
2·$1/2Et_2O$·$1/2C_3H_6O$	−84,[a] −25[b]	−116
Uncomplexed ligand, $Fe[C_5H_4CH(pz)_2]_2$	−35, −27	180
Helical Ag complexes	−72,[c] −65[c]	88[c]
Nonhelical Ag complexes	−71,[c] −63[c]	94[c]

[a] Value for part of compound containing complexed Rhenium atom.
[b] Value for part of compound with uncomplexed pyrazolyl rings.
[c] Average values.

support the three-dimensional structure with each CH_3NO_2 molecule bridging two different chains. Two pyrazolyl ring hydrogen atoms, H(11) and H(21), each from different chains, are directed toward the oxygen atoms, O(41) and O(42), of the same solvent molecule. The H···O distances for these two interactions are 2.59 Å (131°) for H(11)···O(41) and 2.57 Å (148°) for H(21)···O(42).

2.6. Supramolecular structure of *1*·*2CH₃CN*

The solid-state structure of compound **1**·$2CH_3CN$ is isomorphous with that of **1**·$2CH_3NO_2$. The molecular units are held into chains by two series of CH···Br interactions with H(1)···Br and H(4)···Br distances of 2.80 Å (151°) and 2.89 Å (172°) (as in Fig. 9). The chains are held into a three-dimensional network by CH···O interactions with an H···O distance of 2.42 Å (168°) (as in Fig. 10), and each chain is "connected" to its four neighboring diagonal chains. The CH_3CN solvent molecules are highly ordered and participate in CH···N weak hydrogen bonding interactions that support the three-dimensional structure with each CH_3CN molecule bridging two different chains. Two pyrazolyl ring hydrogen atoms, H(21) and H(23), each from different chains, are directed toward the nitrogen atom, N(41), of the

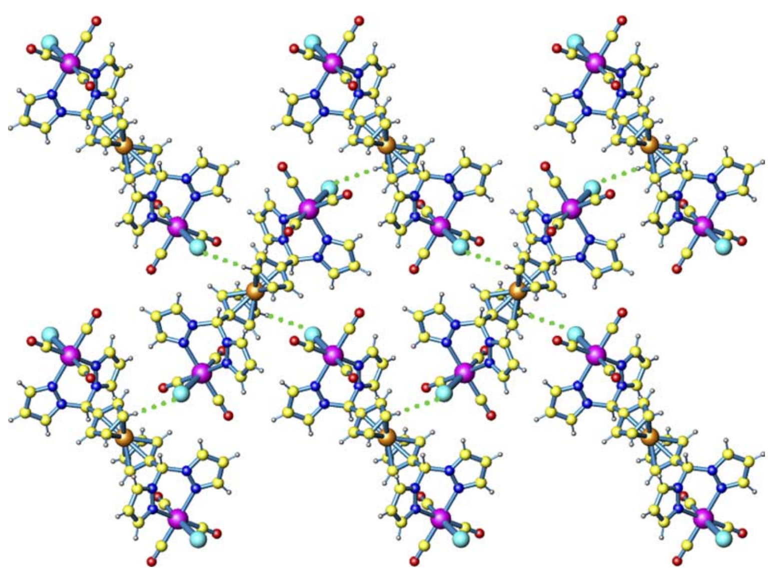

Fig. 7. A two-dimensional sheet of molecular units of **1** · CH_3NO_2 organized by C–H···Br weak hydrogen bonding interactions (green dots).

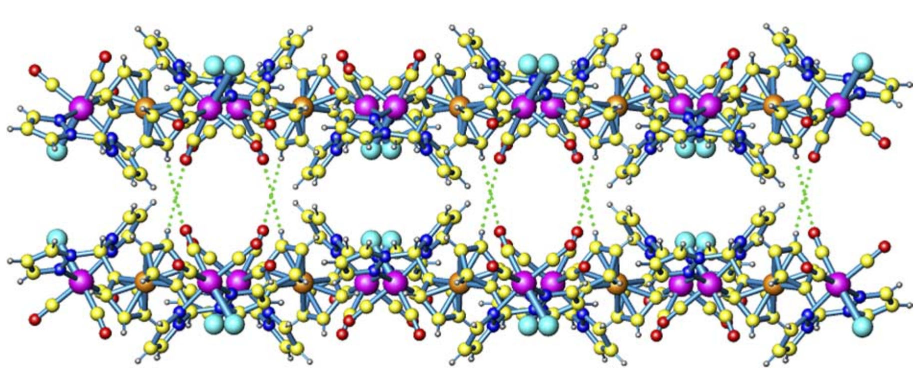

Fig. 8. Two sheets of **1** · CH_3NO_2 organized in a three-dimensional network by C–H···O weak hydrogen bonding interactions (green dots). The disordered CH_3NO_2 molecules are trapped between the sheets, but have been omitted for clarity.

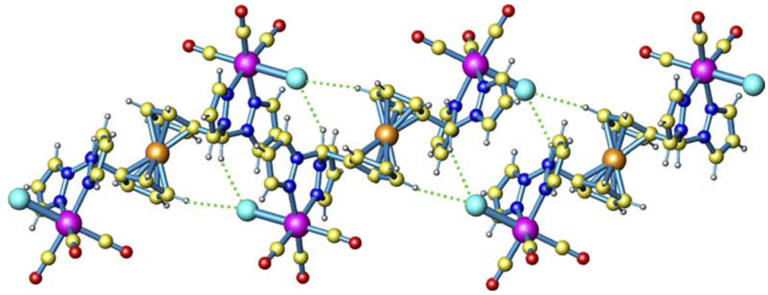

Fig. 9. A chain of three molecules of **1** · $2CH_3NO_2$ organized by C–H···Br weak hydrogen bonding interactions (green dots).

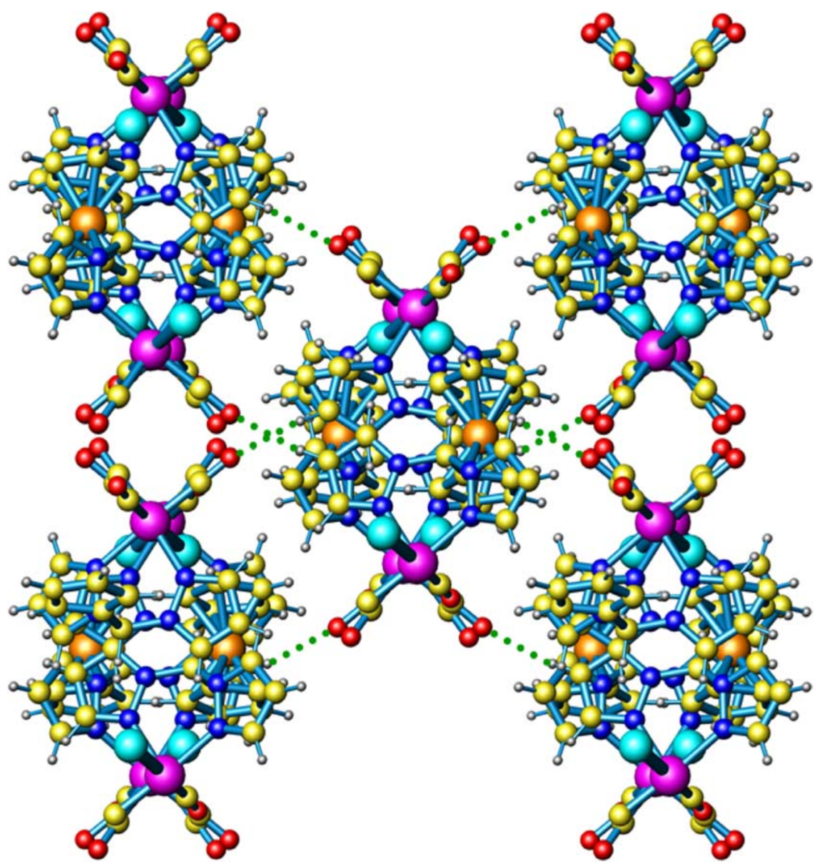

Fig. 10. Five chains (view orthogonal to orientation in Fig. 9) of **1** · $2CH_3NO_2$ organized in a three-dimensional array by a series of C–H···O interactions. For clarity, the non-covalent solvent interactions are not shown.

same solvent molecule. The H···N distances for these two interactions are 2.55 Å (151°) for H(21)···N(41) and 2.60 Å (136°) for H(23)···N(42), and are within the sum of their van der Waals radii (2.74 Å for H···N) [6].

2.7. Supramolecular structure of **2** · 1/2Et_2O · 1/2C_3H_6O

The molecular units of **2**·1/2Et_2O·1/2C_3H_6O are organized into chains via CH···Br and CH···O weak hydrogen bonding interactions (Fig. 11). The acidic methine hydrogen atom from the complexed part of the molecule, H(1), of one unit is directed toward the bromine atom of an adjacent molecule with an H···Br distance of 2.85 Å (162°). In the CH···O interaction, a hydrogen atom, H(58), from the Cp ring is aimed at the oxygen atom, O(61), of a carbonyl ligand from an adjacent unit with an H···O distance of 2.56 Å (156°). These two interactions originate from the same molecule, but are directed towards two different molecules within the chain, which is organized such that each molecular unit interacts non-covalently with four adjacent molecules within the same chain.

The chains are arranged into two-dimensional sheets by CH···N weak hydrogen bonding interactions

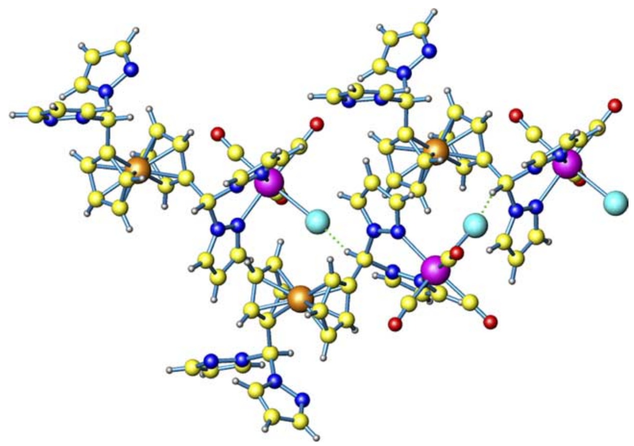

Fig. 11. A chain of three molecules of **2** · 1/2Et_2O · 1/2C_3H_6O organized by C–H···Br and C–H···O weak hydrogen bonding interactions (green dots).

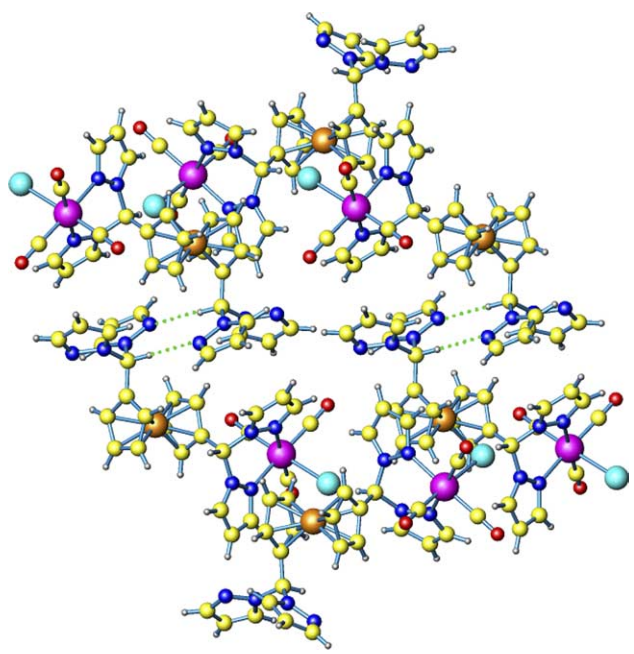

Fig. 12. Two chains of **2** · 1/2Et_2O · 1/2C_3H_6O arranged in a two-dimensional sheet by C–H···N weak hydrogen bonding interactions (green dots).

(Fig. 12). The methine hydrogen atom, H(2), from the part of the molecule containing the uncomplexed bis(pyrazolyl)methane moiety, is directed toward an uncomplexed pyrazolyl ring nitrogen atom, N(31), from an adjacent chain. The H···N distance for this interaction is 2.41 Å (177°).

3. Summary

The dirhenium derivative $Fe[C_5H_4CH(pz)_2Re(CO)_3Br]_2$ (**1**) has been prepared by the reaction of $Fe[C_5H_4CH(pz)_2]_2$ with two equivalents of $Re(CO)_5Br$. While **1** can be synthesized in high yield, the preparation of the mono-rhenium derivative $Fe[C_5H_4CH(pz)_2Re(CO)_3Br][C_5H_4CH(pz)_2]$ (**2**) is less efficient. The low yield is a result of the mono-derivative converting to the bis-derivative at a rate comparable to its own formation and to difficulties associated with its separation from the free ligand whose solubility and retention factors are comparable to those in **2**.

A cyclic voltammetry study of **1** and **2** showed that each compound has one reversible oxidation around 0.90 V and one irreversible oxidation around 1.40 V, which can be assigned to the oxidation of the ferrocene and the rhenium metal center, respectively. The complexation of the rhenium groups to the ligand increases the oxidation potential of the ferrocenyl unit relative to the uncomplexed ligand $Fe[C_5H_4CH(pz)_2]_2$, which shows an irreversible oxidation for its ferrocene moiety at 0.61 V. Coordination of the bis(pyrazolyl)methane units to rhenium makes them a more electron withdrawing substituent on the cyclopentadienyl ring, increasing the ferrocene potential. While complexation of the rhenium groups to the ligand also makes the oxidation reversible, the surprising result is that the wave for the ligand is irreversible. Interestingly, similar irreversible waves were observed with the thallium complexes of the tris(pyrazolyl)borate $Tl_2\{Fe[C_5H_4B(pz)_3]_2\}$, although in these cases the thallium was suggested as the reason for the irreversibility [7]. The oxidation potentials for the rhenium metal center in compounds **1** and **2** are comparable to the values for other analogous bis(pyrazolyl)methane rhenium tricarbonyl bromide complexes; the ferrocene central linker in **1** and **2** has negligible impact on the electronic environment of rhenium.

A comparison of the structures of the free ligand, its silver and rhenium complexes reveals that the relative orientation of the two "arms" of the ligands, τ_2, depends on the crystal packing interactions. Intramolecular steric interactions of the arms within the ferrocenyl moiety do not appear to be important. In the free ligand and the dirhenium complex **1**·CH_3NO_2 the bis(pyrazolyl)methane ligating sites are 180° apart about the ferrocene linker in an antiperiplanar staggered orientation. The arms are closer together at 136° when **1** is crystallized as either a nitromethane or acetonitrile disolvate, where only the number and not the nature of solvent is consequential to the final arrangement. The bis(pyrazolyl)methane moieties in **2**·1/2Et_2O·1/2C_3H_6O are separated by 116°, which puts it and the two bis-solvated compounds of **1** in the ranges of the anticlinal staggered and anticlinal eclipsed orientations. These separations are greater than those for the silver complexes reported earlier which ranged from 88° to 94° depending on both the number of solvent molecules of crystallization and the hydrogen-binding ability of the anions. In all the systems the compounds are held together into elaborate supramolecular structures based on non-covalent interactions such as CH···π, π···π, CH···N, CH···halide or CH···O interactions, where available. A more thorough understanding of these intermolecular forces may ultimately be useful for the deliberate construction of future functional supramolecular systems with controlled 1,1′-ferrocenyl geometries.

4. Experimental

All operations were carried out under a nitrogen atmosphere using either standard Schlenk techniques or a Vacuum Atmospheres HE-493 drybox. All solvents were dried and distilled prior to use. 1,1′-Bis(dipyrazol-1-ylmethyl)ferrocene [1a], $Re(CO)_5Br$ [8], and bis(pyrazol-1-yl)methane [9] were prepared according to literature procedures. Robertson Microlit Laboratories, Inc. (Madison, NJ), performed the elemental analyses. Reported temperatures for melting point determinations are uncorrected. ^1H (400 MHz) and ^{13}C (100.62 MHz) NMR chemical shifts are reported in ppm versus TMS and referenced to the residual solvent peaks for d_6-acetone, δ 2.05 (^1H) and δ 29.9 (^{13}C). Mass spectrometric measurements were obtained on a MicroMass QTOF spectrometer using acetonitrile as the solvent. Electrochemical measurements were collected with a BAS CV-50W instrument at a scan rate of 200 mV/s for samples as 0.1 mM CH_3CN solutions with 0.1 M NBu_4PF_6 as the supporting electrolyte, and a three-electrode cell comprised of a Ag/AgCl reference electrode, a platinum working electrode, and a glassy carbon counter electrode. The reported values were corrected to the ferrocene couple (+0.32 V vs Ag/AgCl) as an external standard.

4.1. Synthesis of $Fe[C_5H_4CH(pz)_2Re(CO)_3Br]_2$ (1)

To a flask containing 1,1′-bis(dipyrazol-1-ylmethyl)ferrocene (0.12 g, 0.25 mmol) and $Re(CO)_5Br$ (0.20 g, 0.50 mmol) was added toluene (20 ml). Upon warming, the mixture became a golden yellow solution, and after heating at reflux for 4 h a yellow precipitate formed. After cooling to room temperature, the colorless solvent was removed via cannula filtration and discarded. The insoluble solid was washed with hexane (2 × 10 ml) and was dried under vacuum to afford the desired compound **1** as a yellow powder (0.27 g, 92%), m.p. 240–245 °C dec. ^1H NMR (d_6-acetone): δ 8.77 (s, 1H, C_α–H), 8.47, 8.12 (d, d, J = 2.0, 1.2 Hz, 2H, 2H,

Table 4
Crystal data and data collection and refinement parameters for compounds **1** · CH_3NO_2, **1** · $2CH_3NO_2$, **1** · $2CH_3CN$ and **2** · $1/2Et_2O$ · $1/2C_3H_6O$

	1·CH_3NO_2	**1** · $2CH_3NO_2$	**1** · $2CH_3CN$	**2**·$1/2Et_2O$ · $1/2C_3H_6O$
Empirical formula	$C_{31}H_{25}Br_2FeN_9O_8Re_2$	$C_{32}H_{28}Br_2FeN_{10}O_{10}Re_2$	$C_{34}H_{28}Br_2FeN_{10}O_6Re_2$	$C_{30.5}H_{30}BrFeN_8O_4Re$
Formula weight	1239.67	1300.71	1260.73	894.59
Temperature (K)	150(1)	200(1)	150(1)	150(1)
Crystal system	Monoclinic	Monoclinic	Monoclinic	Monoclinic
Space group	*C*2/*c*	*C*2/*c*	*C*2/*c*	$P2_1n$
Unit cell dimensions				
a (Å)	19.1782(12)	20.6741(13)	20.4662(10)	11.8815(7)
b (Å)	15.3261(9)	15.0790(10)	14.9191(7)	12.1653(7)
c (Å)	14.5625(9)	13.5020(9)	13.6317(7)	21.8238(12)
α (°)	90	90	90	90
β (°)	121.0700(10)	108.1830(10)	107.7960(10)	94.5220(10)
γ (°)	90	90	90	90
V (Å^3)	3666.2(4)	3999.0(5)	3963.1(3)	3.144.6(3)
Z	4	4	4	4
Density (calcd) (Mg/m^3)	2.246	2.16	2.113	1.89
Absorption coefficient (mm^{-1})	9.219	8.462	8.528	5.628
θ range for data collection (°)	1.82–26.38	1.70–26.38	1.72–27.92	1.87–26.39
No. of reflections collected	15,147	15,992	16,246	25,763
No. of independent reflections (R_{int})	3759 (0.0267)	4080 (0.0328)	4731 (0.0370)	6436 (0.0286)
Completeness to θ_{max} (%)	99.8	100	99.7	100
Absorption correction	Semi-empirical from equivalents			
Max./min. transmission	1.0000/0.4686	1.0000/0.4302	1.0000/0.4241	1.0000/0.7397
No. of data/restraints/parameters	3759/0/255	4080/0/259	4731/0/250	6436/7/399
Goodness-of-fit on F^2	1.07	1.041	1.05	1.065
Final R indices ($I > 2\sigma(I)$)				
R_1	0.0209	0.0224	0.0265	0.0276
wR_2	0.0519	0.0539	0.0627	0.0691
R indices (all data)				
R_1	0.0234	0.0259	0.0313	0.0318
wR_2	0.0528	0.0551	0.0646	0.0712
Largest difference peak/hole (e/Å^3)	1.781/−0.448	1.015/−1.033	1.756/−0.663	1.916/−1.013

$H_{3,5}$–pz), 6.72 (dd, $J = 2.4$, 2.0 Hz, 2H, H_4–pz), 4.48 (m, 2H, Cp–H), 3.97 (m, 2H, Cp–H). IR(CH_3CN, ν(CO)): 2027 cm^{-1} (s), 1921, 1898 cm^{-1} (m). HRMS: ESI^+ (*m/z*): $[M - Br]^+$ calcd. for $[C_{30}H_{22}N_8O_6BrFeRe_2]^+$, 1098.9288, found, 1098.9288. ESI^+ MS *m/z* (Rel. Int. %) [assgn]: 1099 (100) $[M - Br]^+$, 1140 (5) $[M \cdot CH_3CN–Br]^+$. Anal. Calcd. for $C_{30}H_{22}N_8Br_2FeO_6Re_2$: C, 30.57, H, 1.88, N, 9.51. Found: C, 30.90, H, 2.03, N, 9.45. Crystals suitable for X-ray structural studies were obtained by vapor diffusion of diethyl ether into a nitromethane or acetonitrile solution of **1**, giving $\mathbf{1} \cdot CH_3NO_2$ and $\mathbf{1} \cdot 2CH_3NO_2$, or $\mathbf{1} \cdot 2CH_3CN$, respectively.

4.2. $Fe[C_5H_4CH(pz)_2Re(CO)_3Br][C_5H_4CH(pz)_2]$ (2)

To a flask containing 1,1′-bis(dipyrazol-1-ylmethyl)ferrocene (0.10 g, 0.21 mmol) and $Re(CO)_5Br$ (0.068 g, 0.16 mmol) was added toluene (20 ml). Upon warming, the mixture became a yellow–orange solution, and after heating at reflux for 0.5 h an orange–brown precipitate formed. After cooling to room temperature, the yellow–orange solvent was removed via cannula filtration and set aside. The yellow insoluble solid was washed with hexane (1 × 10 ml) and was dried under vacuum to afford **1** (0.078 g, 83%) as shown by ^1H NMR. The hexane washes were combined with the filtrate solution, and upon standing overnight, a yellow precipitate formed. The filtrate solution was decanted and the remaining yellow solid was washed with hexane, collected, and dried under vacuum to give **2** as a yellow powder (0.011 g, 8%), m.p. 162–165 °C dec. ^1H NMR (d_6-acetone) δ 8.76 (s, 1H, C_α–H (Re)), 8.47, 8.09 (s, s, 2H, 2H, $H_{3,5}$–pz (Re)), 7.84, 7.52 (s, s, 2H, 2H, $H_{3,5}$–pz (free)), 7.66 (s, 1H, C_α–H (free)), 6.71 (s, 2H, H_4–pz (Re)), 6.28 (s, 2H, H_4–pz), 4.73, 4.52 (m, m, 2H, 2H, Cp–H (Re)), 4.07, 3.66 (m, m, 2H, 2H, Cp–H (free)). IR(CH_3CN, ν(CO)): 2027 cm^{-1} (s), 1920, 1899 cm^{-1} (m). HRMS: ESI^+ (*m/z*): $[M + H]^+$ calcd for $[C_{27}H_{23}N_8O_3BrFeRe]^+$, 826.9964, found, 826.9976. ESI^+ MS *m/z* (Rel. Int. %) [assgn]: 829 (6) $[M + H]^+$, 761 (96) $[M - pz]^+$, 749 (28) $[M - Br]^+$, 478 (13) $[L]^+$, 411 (100) $[L - pz]^+$. Crystals suitable for X-ray structural studies were obtained by vapor diffusion of diethyl ether into an acetone solution of **2**, giving $\mathbf{2} \cdot 1/2Et_2O \cdot 1/2C_3H_6O$.

4.3. Synthesis of $H_2C(pz)_2Re(CO)_3Br$ (3)

To a flask containing bis(pyrazol-1-yl)methane (0.500 g, 3.37 mmol) and $Re(CO)_5Br$ (1.37 g, 3.37 mmol) was added toluene (50 ml). The mixture was heated at reflux for 3 h, and a white precipitate formed. After cooling to room temperature, the colorless solvent was removed via cannula filtration. The white solid was washed with hexane (1 × 20 ml) and dried under vacuum to afford **3** (1.57 g, 93%). ^1H NMR (d_6-acetone, ambient temperature) δ 8.21, 8.10 (d, d, 2H, 2H, $J = 2.7$, 2.4 Hz, $H_{3,5}$–pz), 7.38, 6.63 (br d, br d, 1H, 1H, $J = 14.7$, 14.4 Hz, H_2C), 6.58 (dd, 2H, $J = 2.7$, 2.4 Hz, H_4–pz), (−75 °C) δ 8.38, 8.27 (d, d, 2H, 2H, $J = 2.0$, 2.4 Hz, $H_{3,5}$–pz minor isomer), δ 8.24, 8.10 (d, d, 2H, 2H, $J = 2.5$, 2.0 Hz, $H_{3,5}$–pz major isomer), 7.64, 7.01 (d, d, 1H, 1H, $J = 14.0$, 14.0 Hz, H_2C minor isomer), 7.28, 6.47 (d, d, 1H, 1H, $J =$ 15.0, 14.5 Hz, H_2C major isomer), 6.67 (dd, 2H, $J = 2.5$, 2.5 Hz, H_4–pz minor isomer), 6.60 (dd, 2H, $J = 2.5$, 2.5 Hz, H_4–pz major isomer). IR(CH_3CN, ν(CO)): 2029 cm^{-1} (s), 1925, 1896 cm^{-1} (m). HRMS: direct probe (*m/z*): [M] calcd for $C_{10}H_8BrN_4O_3Re$, 497.9320, found, 497.9327.

4.4. Crystallographic studies

Single crystals for X-ray diffraction studies were grown for each compound as described above. In the case of **1**, two types of crystals formed from the same stock nitromethane solution. The crystals, $\mathbf{1} \cdot CH_3NO_2$ and $\mathbf{1} \cdot 2CH_3NO_2$, were grown in the same larger vial, but formed in different inner vials. Crystal data and data collection and refinement parameters are given in Table 4.

A yellow needle of $\mathbf{1} \cdot CH_3NO_2$, a yellow plate of $\mathbf{1} \cdot 2CH_3CN$, and a yellow block of $\mathbf{2} \cdot 1/2Et_2O \cdot 1/2C_3H_6O$ were mounted on the ends of thin glass fibers using inert oil and quickly transferred to the diffractometer cold stream for data collection at 150(1) K. A yellow plate of $\mathbf{1} \cdot 2CH_3NO_2$ was also mounted for X-ray data collection at 200(1) K. Raw X-ray intensity data frames were measured on a Bruker SMART APEX CCD-based diffractometer system (Mo Kα radiation, $\lambda = 0.71073$ Å). The raw data frames were integrated using SAINT+ [10], which also applied corrections for Lorentz and polarization effects. Analysis of the data sets showed negligible crystal decay during data collection in any case. An empirical absorption correction based on the multiple measurement of equivalent reflections was applied to each data set with the program SADABS [10]. All structures were solved by a combination of direct methods and difference Fourier syntheses and refined by full-matrix least squares against F^2, using the SHELXTL software package [11]. Non-hydrogen atoms were refined with anisotropic displacement parameters, and hydrogen atoms were placed in geometrically idealized positions and included as riding atoms with refined isotropic displacement parameters.

$Fe[C_5H_4CH(pz)_2Re(CO)_3Br]_2 \cdot CH_3NO_2$ ($\mathbf{1} \cdot CH_3NO_2$) crystallizes with imposed inversion symmetry in the space group *C*2/*c*, with one molecule of nitromethane per formula unit. The Fe atom lies on the inversion center. The nitromethane molecule is disordered about a twofold rotational axis.

$Fe[C_5H_4CH(pz)_2Re(CO)_3Br]_2 \cdot 2CH_3NO_2$ (**1**$\cdot 2CH_3NO_2$) crystallizes with imposed C_2 symmetry in the space group *C*2/*c*, with two molecules of nitromethane per formula unit. The Fe atom lies on the two fold rotational axis.

$Fe[C_5H_4CH(pz)_2Re(CO)_3Br]_2 \cdot 2CH_3CN$ (**1**$\cdot 2CH_3CN$) crystallizes with imposed C_2 symmetry in the space group *C*2/*c*, with two molecules of acetonitrile per formula unit. The Fe atom lies on the twofold rotational axis.

$Fe[C_5H_4CH(pz)_2Re(CO)_3Br][C_5H_4CH(pz)_2] \cdot 1/2Et_2O \cdot 1/2C_3H_6O$ (**2**$\cdot 1/2Et_2O \cdot 1/2C_3H_6O$) crystallizes with no imposed symmetry in the space group $P2_1/n$ as shown by systematic absences in the intensity data. The asymmetric unit contains one $Fe[C_5H_4CH(pz)_2Re(CO)_3Br][C_5H_4CH(pz)_2]$ unit, half of an acetone molecule, and half of a diethyl ether molecule of crystallization disordered in the same region. A disorder model using seven restraints was employed to maintain a reasonable chemical geometry for these species.

5. Supplementary material

Crystallographic data for the structural analysis has been deposited with the Cambridge crystallographic Centre, CCDC No. 247431–247434. Copies of this information may be obtained free of charge from the director, CCDC, 12 Union Road, Cambridge, CB2 1EZ UK (fax +44-1223-336-033; e-mail deposit@ccdc.cam.ac.uk, or www: http://www.ccdc.cam.ac.uk).

Acknowledgement

We thank the National Science Foundation (CHE-0414239) for support. The Bruker CCD Single Crystal Diffractometer was purchased using funds provided by the NSF Instrumentation for Materials Research Program through Grant DMR:9975623. We thank Dr. Radu F. Semeniuc for assistance in preparing the manuscript and Dr. Perry J. Pellechia for assistance in obtaining the variable temperature NMR spectra.

References

[1] (a) D.L. Reger, K.J. Brown, J.R. Gardinier, M.D. Smith, Organometallics 22 (2003) 4973;
(b) D.L. Reger, J.R. Gardinier, R.F. Semeniuc, M.D. Smith, J. Chem. Soc., Dalton Trans. (2003) 1712;
(c) D.L. Reger, T.D. Wright, R.F. Semeniuc, T.C. Grattan, M.D. Smith, Inorg. Chem. 40 (2001) 6212;
(d) D.L. Reger, R.F. Semeniuc, M.D. Smith, Eur. J. Inorg. Chem. (2002) 543;
(e) D.L. Reger, R.F. Semeniuc, M.D. Smith, J. Chem. Soc., Dalton Trans. (2002) 476;
(f) D.L. Reger, R.F. Semeniuc, M.D. Smith, J. Organomet. Chem. 666 (2003) 87;
(g) D.L. Reger, R.F. Semeniuc, I. Silaghi-Dumitrescu, M.D. Smith, Inorg. Chem. 42 (2003) 3751;
(h) D.L. Reger, R.F. Semeniuc, V. Rassolov, M.D. Smith, Inorg. Chem. 43 (2004) 537.

[2] (a) K.S. Gan, T.S.A. Hor, 1,1′-Bis(diphenylphosphino)ferrocene – coordination chemistry, organic syntheses, and catalysis, in: A. Togni, T. Hayashi (Eds.), Ferrocenes: Homogeneous Catalysis, Organic Synthesis, Material Science, VCH, Weinheim, Germany, 1995, pp. 3–104;
(b) R.D.A Hudson, J. Organomet. Chem. 637 (2001) 47;
(c) G. Dong, L. Yu-ting, D. Chun-ying, M. Hong, M. Qing-jin, Inorg. Chem. 42 (2003) 2519.

[3] D.L. Reger, J.R. Gardinier, P.J. Pellechia, M.D. Smith, K.J. Brown, Inorg. Chem. 42 (2003) 7635.

[4] (a) T. Rajendran, B. Manimaran, R.-T. Liao, R.-J. Lin,, P. Thanasekaran, G.-H. Lee, S.-M. Peng, Y.-H. Liu, I.-J. Chang, S. Rajagopal, K.-L. Lu, Inorg. Chem. 42 (2003) 6388;
(b) S.-S. Sun, A.J. Lees, J. Am. Chem. Soc. 122 (2000) 8956;
(c) K.M.-C. Wong, S.C.-F. Lam, C.-C. Ko, N. Zhu, V.W.-W. Yam, S. Roue, C. Lapinte, S. Fathallah, K. Costuas, S. Kahlal, J.-F. Halet, Inorg. Chem. 42 (2003) 7086;
(d) J. Guerrero, O.E. Piro, E. Wolcan, M.R. Feliz, G. Ferraudi, S.A. Moya, Organometallics 20 (2001) 2842;
(e) Y. Hayashi, S. Kita, B.S. Brunschwig, E. Fujita, J. Am. Chem. Soc. 125 (2003) 11976.

[5] L.J. Farrugia, Appl. Cryst. 30 (1997) 565.

[6] (a) A.J. Bondi, Phys. Chem. 68 (1964) 441;
(b) R.S. Rowland, R.J. Taylor, Phys. Chem. 100 (1996) 7384.

[7] F. Fabrizi de Biani, F. Jäkle, M. Spiegler, M. Wagner, P. Zanello, Inorg. Chem. 36 (1983) 2103.

[8] S.P. Schmidt, W.C. Trogler, F. Basolo, Inorg. Syn. 28 (1990) 160.

[9] D.L. Jameson, R.K. Castellano, Inorg. Syn. 32 (1998) 51.

[10] SMART Version 5.625, SAINT+ Version 6.02a and SADABS. Bruker Analytical X-ray Systems, Inc., Madison, WI, USA, 1998.

[11] G.M. Sheldrick, SHELXTL Version 5.1, Bruker Analytical X-ray Systems, Inc., Madison, WI, USA, 1997.